Nonuniform Composition Profile in $In_{0.5}Ga_{0.5}As$ Alloy Quantum Dots

N. Liu,[1] J. Tersoff,[2] O. Baklenov,[3] A. L. Holmes, Jr.,[3] and C. K. Shih[1]

[1]*Department of Physics, The University of Texas, Austin, Texas 78712*
[2]*IBM Research Division, T. J. Watson Research Center, P.O. Box 218, Yorktown Heights, New York 10598*
[3]*Department of Electrical and Computer Engineering, The University of Texas, Austin, Texas 78712*
(Received 12 July 1999)

We use cross-sectional scanning tunneling microscopy to examine the shape and composition distribution of $In_{0.5}Ga_{0.5}As$ quantum dots (QDs) formed by capping heteroepitaxial islands. The QDs have a truncated pyramid shape. The composition appears highly nonuniform, with an In-rich core having an inverted-triangle shape. Thus the electronic properties will be drastically altered, relative to the uniform composition generally assumed in device modeling. Theoretical analysis of the QD growth suggests a simple explanation for the unexpected shape of the In-rich core.

Strain-driven self-assembly of semiconductor quantum dots (QDs) has recently attracted tremendous attention, opening up a new dimension in nanoengineering of materials for electronic and optoelectronic applications [1–3]. This approach reverses the traditional paradigm of thin film growth. Instead of attempting to suppress growth of three-dimensional (3D) islands, it exploits island formation to form nanoscale semiconductor QDs with desired electronic properties.

Many theoretical [4–6] and experimental [7–12] efforts have investigated how different growth parameters influence the size, shape, and composition of QDs, in the hope that such understanding will allow better control of the electronic properties. However, despite some recent progress, there has been relatively little direct information regarding the alloy composition of quantum dots and its uniformity and distribution within the dot.

Yet the composition distribution is critical for device design, since it is ultimately this which controls the operation of QD devices. After capping, electrons and holes are not confined by any structural boundary, only by composition gradients. Therefore, if the composition varies within a QD, the effective confining potential may bear little resemblance to the shape of the island.

Here we report cross-sectional scanning tunneling microscopy (STM) studies of the shape and compositional inhomogeneity of $In_{0.5}Ga_{0.5}As$ QDs. We find that these QDs have (i) a truncated pyramid shape with well-defined facets and (ii) an In-rich core having an inverted-triangle shape, with its (downward-pointing) apex at the center of the island base. This unexpected In distribution implies that the *effective* shape of the QD is entirely different than expected, having smaller size (and presumably a higher In fraction) than would be supposed. Thus knowledge of the composition distribution is indeed essential for device design and modeling.

Theoretical arguments can account for the unexpected composition profile. With reasonable assumptions about the growth mode, scaling arguments predict a compositionally enriched core with inverted-triangle shape, for any

island shape. We therefore believe that the results here represent a rather general phenomenon. In addition, we present an explicit calculation of the composition distribution within a simplified model.

$In_{0.5}Ga_{0.5}As$ QDs were grown on GaAs (001) using migration enhanced epitaxy (MEE), a refined molecular beam epitaxy (MBE) technique [2,13]. During growth of $In_{0.5}Ga_{0.5}As$ QDs the temperature is maintained at 510 °C, while In and Ga are supplied alternately in discrete increments of 0.5 monolayer (ML), each followed by 7 s As flux. This approach gives enhanced migration lengths of In and Ga in the absence of As, leading to the formation of larger QDs. The GaAs capping layer was grown at 600 °C, with continuous Ga and As fluxes.

Samples were cleaved *in situ* in the STM chamber (base pressure $<4 \times 10^{-11}$ torr) to expose (110) and ($1\bar{1}0$) cleavage faces normal to the growth surface. Such a "cross-sectional surface" exposes the buried structure. Since the sample is cleaved at room temperature, atomic mobility is negligible, so the image reveals the structure without disturbing it.

Figure 1(a) is a STM image [on (110) surface] of a sample consisting of three stacks of $In_{0.5}Ga_{0.5}As$, grown by MEE on GaAs (001). Each stack contains the equivalent of 10 ML of alloy, in the form of islands on a thin wetting layer. Two factors contribute to the contrast of the image: (i) outward strain relaxation [14,15], forming topographic protrusions on the surface; (ii) electronic effect [16–18]. Both effects cause In-rich regions to appear brighter than Ga-rich regions—the larger size of In causes outward relaxation, while the smaller band gap gives increased current.

The QDs exhibit a trapezoidal shape, with well-defined sidewall facets about 35° with respect to the base of the QD, and a flat (001) facet on top. Many stacks of 10 ML QDs have been studied. Although they exhibit some variations in sizes [with an average base length of 45 nm and an average height of 10 nm on the (110) surface], each of them has the same sidewall facets.
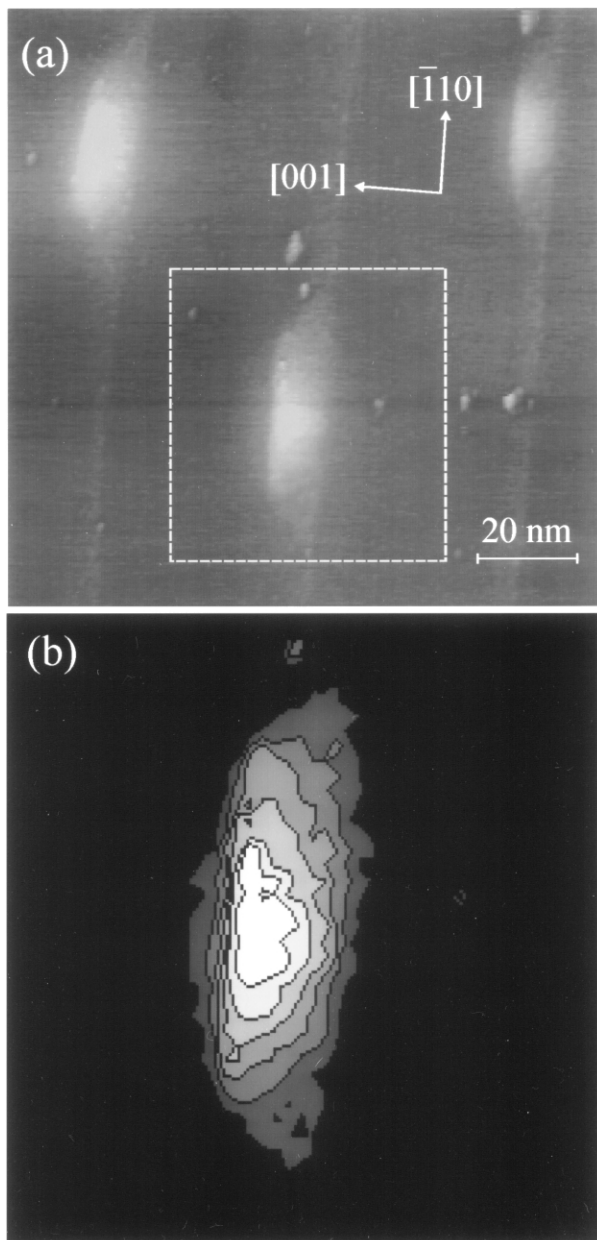
FIG. 1.   (a) A 120 nm × 120 nm STM image obtained from (110) cleavage surface. The growth surface is toward the left. Within a QD the bright triangular shape with the base at the top of the dot indicates the nonuniform distribution of In atoms. The gray scale displayed is 5.5 Å.   (b) Contour plot of the middle QD [frame marked in (a)]; contour intervals are 0.5 Å.

From Fig. 1(a), one can also see that inside a QD the bright region forms roughly an inverted triangle with its apex at the center of the island base, indicative of a highly nonuniform distribution of In atoms. Figure 1(b) is a contour plot illustrating the transition from the inverted-triangle shape of the In-rich core region to the trapezoidal shape of the QD perimeter. Quantitative interpretation of the contrast would be difficult, due to the existence of outward strain relaxation after cleaving [14,15]. Nevertheless, one may generally associate higher

brightness in the gray scale with In enrichment. For a uniform composition, the elastic displacement should be larger at the center of the island base than at the top, so the observed (opposite) behavior must reflect the nonuniform composition.

Similar results are obtained on the $(1\bar{1}0)$ surface: a trapezoidal shape of the QD perimeter and an inverted-triangle shape of the In-rich core [see Fig. 2(a)]. However, on the $(1\bar{1}0)$ projection, these QDs have a longer base length (61 nm on average), and a smaller facet angle of about 25°. The facet angle is consistent with the conclusion using the chevron patterns in reflection high-energy electron diffraction with the electron beam incident along the $[1\bar{1}0]$ azimuth during the growth [13,19]. An anisotropic shape was also observed by Guha *et al.* [20] for MBE-grown $In_{0.5}Ga_{0.5}As$ QDs using transmission electron microscopy, and we suppose that it reflects the anisotropic surface energy. As both projections, (110) and $(1\bar{1}0)$, exhibit an In-rich core with inverted-triangle shape, we conclude that this core has roughly an inverted-pyramid or inverted-cone shape, with its (downward-pointing) apex at the center of the island base. Measurements performed on MEE-grown 15 ML QDs exhibit the same inverted-triangle shape of In-rich core.

The distribution of [001] lattice spacings is also consistent with this shape for the concentration profile. Figure 2(a) shows an STM image on a $(1\bar{1}0)$ surface with atomic resolution; three directions in the image are indicated by arrows. Figure 2(b) shows a closeup view of the region along direction M and its corrugation profile (background subtracted), illustrating how we extract the local lattice constant. Figure 2(c) gives the [001] lattice spacing, determined in this way, along the three indicated directions: across the side (labeled as S), the middle (M), and the center (C) of the QD. Some data points are missing in the C region because the signal to noise is too low to allow such a determination.

In Fig. 2(c) the GaAs matrix exhibits visible compressive strain along [001] both underneath and above the QD, presumably caused by the lateral tensile strain. The strained region extends 2–3 nm into the GaAs, and the magnitude of strain increases from the side to the center of the QD. The [001] lattice spacing inside the QD shows a complicated structure: high at the base and top of the QD with a dip in the middle. Such an M-shaped profile has been reported by Legrand *et al.* [21], for MBE-grown InAs QDs in the GaAs matrix.

The average lattice spacing in the QD shows an increasing trend from the S region to the C region. Taking the first six unit cells from the base as an average, the average lattice spacings are 5.86, 5.98, and 6.06 ± 0.1 Å for the S, M, and C regions, respectively, implying an increase in In concentration from the side to the center of the QD. Consistent with this trend, one also observed the increasing trend in the compressive strain of the
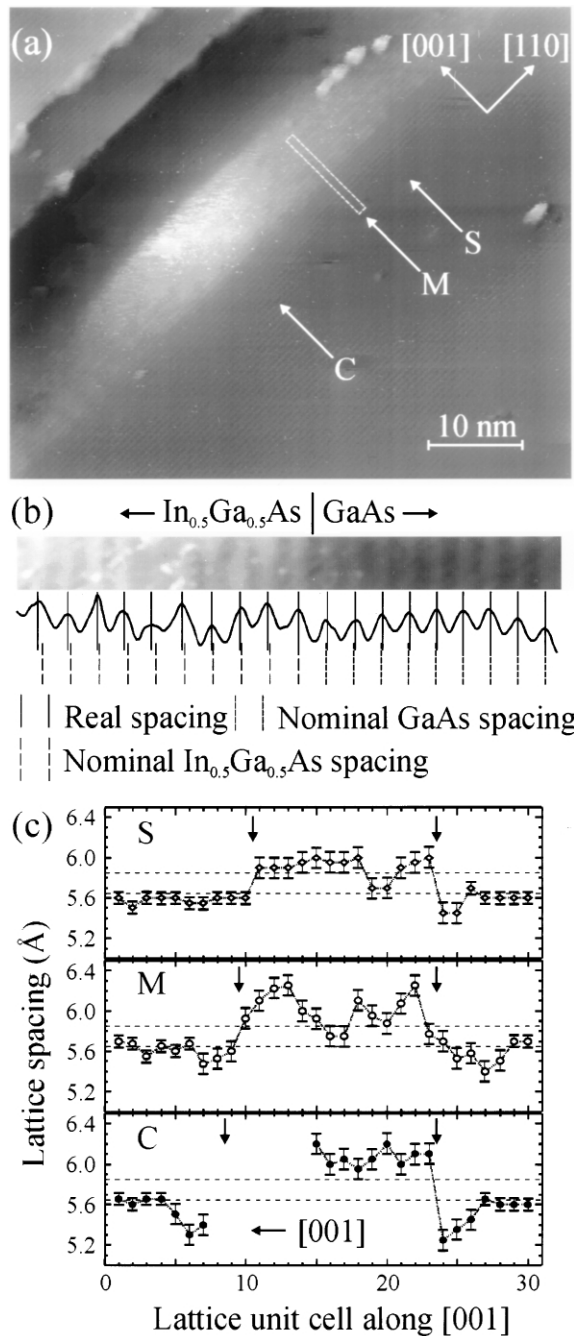
FIG. 2.   (a) A 60 nm × 50 nm STM image of QD obtained from $(1\bar{1}0)$ surface.   (b) A zoom-in view along the M section of the QD (frame marked) in (a) and its corrugation profile with background subtraction.   (c) Profiles of the lattice spacing determined along three directions marked in the STM image. Each unit along the [001] direction corresponds to 2 ML since only every other layer is observed on the (110) or $(1\bar{1}0)$ surface. The arrows (pointing downward) indicate the top (left) and the base (right) of the QD.   The upper and lower dashed lines indicate the nominal spacing lattices for $In_{0.5}Ga_{0.5}As$ and GaAs, respectively.

GaAs region beneath the base.   All these behaviors are consistent with the interpretation of an inverted-triangle shape In-rich region in the core.

We believe that the inverted-triangle composition profile has a very simple and general origin.   Let us assume that the island grows with a fixed shape, and with negligible bulk diffusion, so the composition at any interior point is fixed at the time when that point lay at the surface.   If material of fixed composition c is slowly added to the island, it will incorporate nonuniformly due to the variation in strain across the island surface. This strain distribution is independent of island size; the surface strain depends only on the scaled position, i.e., on the angle relative to the center of the base (see Fig. 3). The contours of constant alloy composition will then be lines radiating from the center of the island base.   This feature will be unaffected even if material is removed from the islands during subsequent capping [8,9,22]. And because the decomposition is independent of size, it preserves the scaling.

Thus a few rather generic assumptions lead immediately to an inverted-triangle profile for the alloy composition.   The argument applies for any island shape, and is unaffected by elastic anisotropy.   The real island-growth and capping processes are doubtless more complex; and other growth modes could give, e.g., radial composition gradients [4].   Nevertheless, this simple picture immediately accounts for the key features of the observed composition distribution.

To provide an explicit calculation of the composition profile, we further simplify the problem by neglecting any additional changes in stress caused by alloy decomposition.   We evaluate the strain within the small-slope approximation [23] and treat the problem in two dimensions for simplicity, assuming that the island grows as a triangle which is truncated during the capping process [8,9,22]. (An alternate shape is considered below.)   Because of these approximations, our treatment cannot be viewed as a
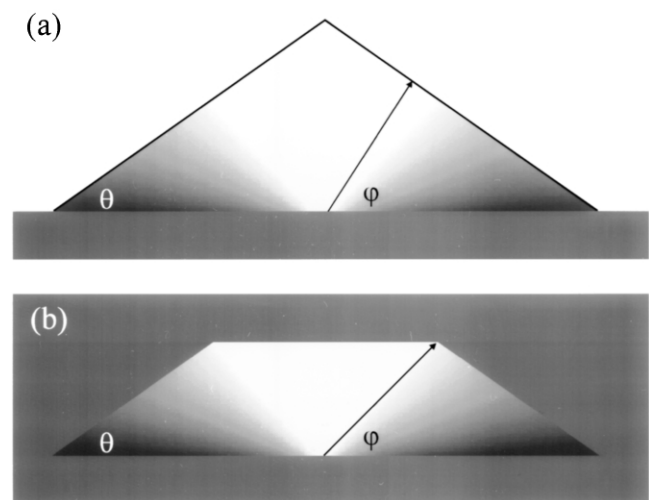

FIG. 3.   Theoretical concentration profiles [Eq. (2)] displayed in gray scale.   (a) Triangular island.   (b) Buried quantum dot. We assume that capping simply dissolves the island apex and surrounds the dot with GaAs.

quantitative description of the real growth process. Nevertheless it illustrates the qualitative behavior.

Within the approximations above, the strain distribution at the island surface is

$$\varepsilon = \bar{\varepsilon} - \beta s \ln(\alpha^2 - 1). \qquad (1)$$

Here β is a ratio of elastic constants of order unity, $\bar{\varepsilon}$ is the misfit strain of a planar layer at the average composition, $s = \tan\theta$ is the facet slope, and $\alpha = 1 + \tan\varphi\cot\theta$, where φ is the angle of the point in question relative to the center of the island base, and both angles are illustrated in Fig. 3. (The logarithmic divergence represents a breakdown of the linear approximation near the island corners but is unimportant for the overall qualitative behavior.)

The equilibrium surface composition is obtained by requiring that the chemical-potential difference between the two constituents be constant across the island surface, giving

$$c = \bar{c} + \lambda s \ln(\alpha^2 - 1), \qquad (2)$$

where λ is proportional to the atomic size difference of the two components and inversely proportional to G'' (the second derivative of the free energy of mixing with respect to composition). Details will be given elsewhere. Note that the decomposition will be particularly strong near the critical temperature for spinodal decomposition, at which G'' vanishes.

As the island grows, points on the surface are buried, so in the absence of bulk diffusion they retain this composition. The resulting concentration profile is displayed in Fig. 3. One can immediately see the inverted-triangle shape of the In-rich core. While this calculation assumed a specific island shape, we emphasize that the inverted-triangle form of the composition profile is quite general. For example, for a platelet shape we obtain

$$c = \bar{c} - \lambda 2 r^3 \cot^2\varphi, \qquad (3)$$

where r is the height/width ratio. While the composition profile depends on island shape, within a specific island the composition is a function only of the angle φ.

Finally, we note that in previous studies, indirect analyses have suggested a gradient of decreasing In fraction from center to edge [7] or top to bottom [12] of the island. Our measurements and calculations are consistent with these suggestions, while explaining more fully the nature and origin of the composition gradients.

In conclusion, we use cross-sectional scanning tunneling microscopy to study MEE-grown $In_{0.5}Ga_{0.5}As$ QDs. We find that while these QDs have a truncated pyramid shape the In-rich core actually resembles an *inverted* pyramid or cone. The distribution of local lattice spacing along the [001] direction is also consistent with such a core. Theoretical analysis suggests that this pattern of decomposition may be a rather general phenomenon in self-assembled quantum dots.

---

[1] For example, see Phys. Today **49**, No. 5, 22 (1996); Mater. Res. Bull. **23**, No. 2, 31 (1998), and references therein.

[2] D. Leonard, M. Krishnamurthy, C. M. Reaves, S. P. Denbaars, and P. M. Petroff, Appl. Phys. Lett. **63**, 3203 (1993).

[3] H. Ishikawa, H. Shoji, Y. Nakata, M. Sugawara, M. Egawa, N. Otsuka, Y. Sugiyama, T. Futatsugi, and N. Yokoyama, J. Vac. Sci. Technol. A **16**, 794 (1998).

[4] J. Tersoff, Phys. Rev. Lett. **81**, 3183 (1998).

[5] István Daruka and Albert-László Barabási, Phys. Rev. Lett. **79**, 3708 (1997).

[6] V. A. Shchukin, N. N. Ledentsov, P. S. Kop'ev, and D. Bimberg, Phys. Rev. Lett. **75**, 2968 (1995).

[7] X. Z. Liao, J. Zou, D. J. H. Cockayne, R. Leon, and C. Lobo, Phys. Rev. Lett. **82**, 5148 (1999).

[8] J. M. García, G. Medeiros-Ribeiro, K. Schmidt, T. Ngo, J. L. Feng, A. Lorke, J. Kotthaus, and P. M. Petroff, Appl. Phys. Lett. **71**, 2014 (1997).

[9] P. Sutter and M. G. Lagally, Phys. Rev. Lett. **81**, 3471 (1998).

[10] U. Woggon, W. Langbein, J. M. Hvam, A. Rosenauer, T. Remmele, and D. Gerthsen, Appl. Phys. Lett. **71**, 377 (1997).

[11] P. D. Siverns, S. Malik, G. McPherson, D. Childs, C. Roberts, R. Murray, and B. A. Joyce, Phys. Rev. B **58**, R10 127 (1998).

[12] A. Rosenauer, U. Fischer, D. Gerthsen, and A. Förster, Appl. Phys. Lett. **71**, 3868 (1997).

[13] R. P. Mirin, J. P. Ibbetson, K. Nishi, A. C. Gossard, and J. E. Bowers, Appl. Phys. Lett. **67**, 3795 (1995).

[14] Huajie Chen, R. M. Feenstra, R. S. Goldman, C. Silfvenius, and G. Landgren, Appl. Phys. Lett. **72**, 1727 (1998).

[15] H. Eisele, O. Flebbe, T. Kalka, C. Preinsberger, F. Heinrichsdorff, A. Krost, D. Bimberg, and M. Dähne-Prietsch, Appl. Phys. Lett. **75**, 106 (1999).

[16] Warren Wu, Jon R. Tucker, Glenn S. Solomon, and James S. Harris, Jr., Appl. Phys. Lett. **71**, 1083 (1997).

[17] N. Liu, C. K. Shih, J. Geisz, A. Mascarenhas, and J. M. Olson, Appl. Phys. Lett. **73**, 1979 (1998).

[18] M. Pfister, M. B. Johnson, S. F. Alvarado, and H. W. M. Salemink, Appl. Phys. Lett. **67**, 1459 (1995).

[19] Y. Nabetani, T. Ishikawa, S. Noda, and A. Sasaki, J. Appl. Phys. **76**, 347 (1994).

[20] S. Guha, A. Madhukar, and K. C. Rajkumar, Appl. Phys. Lett. **57**, 2110 (1990).

[21] B. Legrand, B. Grandidier, J. P. Nys, D. Stiévenard, J. M. Gérard, and V. Thierry-Mieg, Appl. Phys. Lett. **73**, 96 (1998).

[22] P. Sutter, E. Mateeva, and M. G. Lagally, J. Vac. Sci. Technol. B **16**, 1560 (1998).

[23] J. Tersoff and R. M. Tromp, Phys. Rev. Lett. **70**, 2782 (1993).